DOI: 10.1002/ejoc.200600460

The Effects of Fluorine and Chlorine Substituents across the Fjords of Bifluorenylidenes: Overcrowding and Stereochemistry

Sergey Pogodin,[a] Ian D. Rae,[b] and Israel Agranat*[c]

Keywords: DFT calculations / (*E*)/(*Z*) isomerization / Bistricyclic aromatic enes / ^{19}F NMR spectroscopy / Through-space coupling / Strained ethylenes

The bistricyclic aromatic enes (BAEs) (*E*)- and (*Z*)-1,1′-difluorobifluorenylidene, 1,8,1′,8′-tetrafluorobifluorenylidene, (*E*)- and (*Z*)-3,3′-difluorobifluorenylidene, 3,6,3′,6′-tetrafluorobifluorenylidene, and their chlorinated analogues were subjected to a DFT study of overcrowding in their *fjord* regions. The B3LYP hybrid functional was employed to calculate energies and geometries of the twisted conformations of these BAEs. The diastereomers **E11′F2** and **Z11′F2** have identical twist angles (ω = 37.1°) and similar degrees of overcrowding, but differ in the degree and mode of pyramidalization, χ. In **E11′F2**, $\chi(C^9) = +\chi(C^{9'})$ = 7.0° (*syn*-pyramidalization), while in **Z11′F2**, $\chi(C^9) = -\chi(C^{9'})$ = 1.0° (*anti*-pyramidalization). By contrast, in **E11′Cl2** and **Z11′Cl2**, ω = 40.6° and 42.7°, respectively. Introducing four halogen substituents results in higher twist angles: ω = 40.3° in **181′8′F4** and 52.6° in **181′8′Cl4**. Surprisingly, **Z11′F2** is more stable than **E11′F2** (ΔH_{298} = –1.9 kJ/mol), whereas **Z11′Cl2** is less stable than **E11′Cl2** (ΔH_{298} = 2.2 kJ/mol). Both results are consistent with the experimental relative stabilities of these diastereomers. The unexpected stability of **Z11′F2** is explained by a combination of steric and electronic effects. Calculations of Coulomb energies for point charge systems of atoms C, F, and H in the *fjord* regions shows stabilization of the (*Z*) diastereomer by –45.5 kJ/mol. The dipole–dipole interactions in the *fjord* region destabilize **Z11′F2** by 6.4 kJ/mol relative to **E11′F2**. Careful examination of the NMR spectra of **E11′F2** and **Z11′F2** shows, in the latter, evidence of long-range fluorine–fluorine coupling over seven bonds (11.4 Hz) and carbon–fluorine coupling over six bonds (4.8 Hz).

Introduction

The bistricyclic aromatic enes (BAEs)[1,2] (Figure 1) have fascinated chemists since bifluorenylidene (**BF**) (Figure 1; X, Y: –) was synthesized in 1875, dixanthylene (Figure 1, X,Y: O) was synthesized in 1895, and thermochromism[3] and photochromism were revealed in bianthrone (Figure 1; X, Y: C=O).[4] They can be classified into *homomerous* bistricyclic aromatic enes (Figure 1, X = Y) and *heteromerous* bistricyclic aromatic enes (Figure 1, X ≠ Y).[5] They may be viewed as bridged tetraarylethylenes or as tetrabenzofulvalenes. These systems are attractive substrates for the study of the ground-state conformations and dynamic stereochemistry of overcrowded polycyclic aromatic enes (PAEs).[4] Thermochromic and photochromic polycyclic aromatic enes are candidates for potential molecular switches.[6]

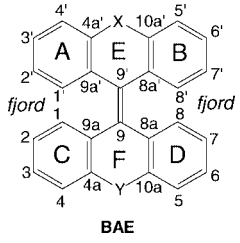

Figure 1. Bistricyclic aromatic enes.

The BAEs, including **BF**, are overcrowded in the *fjord* regions on both sides of the central ene (C^9=$C^{9'}$). Intramolecular overcrowding is a steric effect shown by aromatic structures in which certain (intramolecular) distances between nonbonded atoms are smaller than the sum of the van der Waals radii of the atoms involved.[4] The intramolecular overcrowding in BAEs requires out-of-plane deformations to alleviate prohibitively close contacts of nonbonded atoms in the *fjord* regions resulting from the sterically demanding tricyclic moieties.

[a] Department of Organic Chemistry, The Hebrew University of Jerusalem,
Jerusalem 91904, Israel
E-mail: sergey@vms.huji.ac.il
[b] Department of History and Philosophy of Science, University of Melbourne,
Victoria 3010, Australia
E-mail: idrae@unimelb.edu.au
[c] Department of Organic Chemistry, The Hebrew University of Jerusalem,
Jerusalem 91904, Israel
E-mail: isria@vms.huji.ac.il
Supporting information for this article is available on the WWW under http://www.eurjoc.org or from the author.

Bifluorenylidene (**BF**), the smallest BAE, is a unique case among the homomerous bistricyclic enes, because of its central five-membered rings, which increase the coplanar distances 1–1′ and 8–8′ compared to those in their central six-membered ring analogues, the bianthracenylidenes. This topology introduces a bias towards planarity of the tricyclic moieties, while concomitantly rendering them sterically less demanding, especially in twisted conformations.[2] Indeed, bifluorenylidenes (BFs) adopt twisted conformations.[7–9] In the parent **BF**, the pure twist around $C^9=C^{9'}$ is 32°.[8] **BF** is a fullerene fragment and a starting material for the preparation of buckybowls.[10,11] As to the question of thermochromism of **BF**, it has been claimed that **BF** "is intensely red, but loses its color when chilled to low temperatures, the same phenomenon as in the case of dixanthylene may be assumed to occur, but in different temperature range".[12] However, this claim of thermochromic character of bifluorenylidene has never been substantiated.

The use of the term *fjord* needs a clarification. The term *fjord* in BAEs was coined in analogy to its use in polycyclic aromatic hydrocarbons (PAHs). The most important overcrowding motifs in PAHs and in BAEs are *bay*, *cove* and *fjord*.[13–16] These well-established terms[13–16] refer to parts of the peripheries of PAHs consisting of three, four and five consecutive C–C bonds, respectively, forming peripheral concave regions. *Bay* is the overcrowding region ($C^4C^{4a}C^{4b}C^5$) in phenanthrene. *Cove* is the overcrowding region ($C^{12}C^{12a}C^{12b}C^{12c}C^1$) in benzo[*c*]phenanthrene ([4]helicene). *Fjord* is the overcrowding region ($C^{14}C^{14a}C^{14b}C^{14c}C^{14d}C^1$) in dibenzo[*c*,*g*]phenanthrene ([5]-helicene). These motifs play a significant role in the mechanisms of carcinogenicity of PAHs, e.g., the *bay*-region diol epoxide theory.[17] Dibenzo[*a*,*l*]pyrene,[18,19] one of the worst environmental hazards,[20,21] has a *cove* region and is chiral, while the notorious carcinogen benzo[*a*]pyrene[22] has a *bay* region and is planar.[23] Kresmar et al.[24] have mistakenly used the term *cove* instead of the preferred term *fjord* to denote the overcrowding regions in bifluorenylidenes. There seems to be no need for more "catchy" nomenclature when the older "*fjord*" can aptly describe such regions in a range of molecules.

We report here the results of a theoretical DFT study of various difluoro-, tetrafluoro-, dichloro- and tetrachlorobifluorenylidenes. An ^{19}F NMR study of the through-space spin–spin interactions in (*E*)- and (*Z*)-1,1′-difluorobifluorenylidenes is also described. Through-space ^{19}F–^{19}F coupling was reported in the literature.[24,25] Special emphasis is given to the effects of fluorine vs. chlorine substituents across the *fjord* regions of bifluorenylidenes and to (*E*) vs. (*Z*) diastereomers. In particular, the unexpected higher stability of the (*Z*)-1,1′-difluoro diastereomer relative to the (*E*)-1,1′-difluoro diastereomer is highlighted and analyzed.

The substitution of hydrogen atoms of **BF** by fluorine and chlorine atoms was primarily motivated by the following considerations. Sterically, but not electronically, fluorine resembles hydrogen: it is the second smallest atom after hydrogen (discarding isotopes). Their van der Waals radii are 115 pm (H) and 140 pm (F).[32] Hence, introducing fluorine atoms in the *fjord* regions (1, 1′, 8, and 8′ positions) was not expected to affect significantly the overcrowding of **BF**. On the other hand, it would allow the use of ^{19}F NMR spectroscopy for studying (*E*)- and (*Z*)-1,1′-difluorobifluorenylidenes and the through-space interactions in their *fjord* regions. By contrast, introducing the bulkier chlorine atom (van der Waals radius 190 pm[32]) in the *fjord* regions was expected to increase the degree of overcrowding. The structures of perchlorobifluorenylidene and 1,3,6,8,1′,3′,6′,8′-octachlorobifluorenylidene, in which all four positions at the *fjord* regions are occupied by chlorine atoms, have been described.[26] For comparison, fluorine and chlorine atoms were also introduced not in the *fjord* regions of **BF** (positions 3, 3′, 6, and 6′). In these substituted bifluorenylidenes overcrowding was not expected to be affected.

Results and Discussion

DFT can be successfully used to probe the aromaticity of large molecular systems, in a cost-effective way, using the different energetic, geometrical and magnetic criteria of aromaticity.[27] Recently, the B3LYP hybrid functional was successfully employed to treat BAEs,[28] LPAHs,[16] fullerenes, and fulvalenes.[29] The following difluoro-, tetrafluoro-, dichloro-, and tetrachlorobifluorenylidenes were subjected to DFT B3LYP calculations, along with the parent bifluorenylidene (**BF**): (*E*)-1,1′-difluorobifluorenylidene (**E11′F2**),[25,30] (*Z*)-1,1′-difluorobifluorenylidene (**Z11′F2**),[25,30] 1,8,1′,8′-tetrafluorobifluorenylidene (**181′8′F4**), (*E*)-3,3′-difluorobifluorenylidene (**E33′F2**), (*Z*)-3,3′-difluorobifluorenylidene (**Z33′F2**), 3,6,3′,6′-tetrafluorobifluorenylidene (**363′6′F4**), (*E*)-1,1′-dichlorobifluorenylidene (**E11′Cl2**),[30] (*Z*)-1,1′-dichlorobifluorenylidene (**Z11′Cl2**),[30] 1,8,1′,8′-tetrachlorobifluorenylidene (**181′8′Cl4**), (*E*)-3,3′-dichlorobifluorenylidene (**E33′Cl4**), (*Z*)-3,3′-dichlorobifluorenylidene (**Z33′Cl2**), and 3,6,3′,6′-tetrachlorobifluorenylidene (**363′6′Cl4**). In the present study, only the twisted conformations were considered.

The structures and atom labeling of the above BFs are shown in Figure 2. Table 1 gives the calculated relative energies [ΔE_{Tot}, ΔH_{298} and ΔG_{298} at the B3LYP/6-31G(d), B3LYP/6-31+G(d), B3LYP/6-311G(d,p) and B3LYP/6-311++G(d,p) levels] of the various twisted BFs under study, along with their symmetries. The respective calculated total energies are given in the Supporting Information (Table S1). Table 2 gives the relative energies of a series of homodesmotic reactions of the studied BFs. Table 3 gives representative optimized geometrical parameters of the twisted conformations of the various BFs under study [at the B3LYP/6-311++G(d,p) level] and the respective experimental parameters of **Z11′F2**,[24] **Z11′Cl2**,[31] and 1,3,6,8,1′,3′,6′,8′-octachlorobifluorenylidene (**13681′3′6′8′Cl8**)[26] derived from their molecular (X-ray) structures. The following geometrical parameters were included: pure ethylenic twist angle[4] (ω) around $C^9=C^{9'}$, defined as the average of the two torsion angles C^{9a}–C^9–$C^{9'}$–$C^{9a'}$ and C^{8a}–C^9–$C^{9'}$–$C^{8a'}$; folding dihedral angle of the tricyclic (fluorenylidene) moiety

(*A–B*), defined as the dihedral angle between the least-square planes of the atoms C^1, C^2, C^3, C^4, C^{4a}, C^{9a} and C^5, C^6, C^7, C^8, C^{8a}, C^{4b} (Figure 2) of the benzene rings and reflecting the nonplanarity of the tricyclic moieties; twisting dihedral angle between the fluorenylidene moieties (*AEB–CFD*), defined as the dihedral angle between the least-square planes of all the untagged and all the tagged carbon atoms; pyramidalization angles[4] (χ) at C^9 and $C^{9'}$, defined as the improper torsion angle C^{9a}–C^9–$C^{9'}$–C^{8a} subtracted from 180°, bond lengths $r(C^9–C^{9'})$, $r(X^1–C^1)$, interatomic nonbonding distances $r(C^1\cdots C^{1'})$, $r(H^8\cdots H^{8'})$, $r(X^1\cdots X^{1'})$, $r(X^1\cdots C^{1'})$, $r(X^1\cdots H^{8'})$ and $r(C^8\cdots H^{8'})$, where X = F or Cl. Additional geometrical parameters are provided in Table S2. Table S3 gives the calculated natural atomic charges at the B3LYP/6-311++G(d,p) level of the various BFs under study. The respective Mulliken charges are given in Table S4. The following analysis is based on the B3LYP/6-311++G(d,p) results.

Geometries

The DFT-calculated geometries of **Z11′F2**, **Z11′Cl2**, and **181′8′Cl4** are in reasonably good agreement with the experimental X-ray molecular structures (Table 3). The slightly smaller experimental twist of **Z11′Cl2** (40.4° vs. 42.7°) and, consequently shorter $Cl^1\cdots Cl^{1'}$ and $Cl^1\cdots C^{1'}$ distances, stem probably from solid-state effects and from intermolecular interactions in the crystal structure. Thus, four chlorine atoms of **Z11′Cl2** form a chain with an intermolecular $Cl^1\cdots Cl^1$ <error>((<=AUTHOR: Cl^1 twice ok?))</error> distance of 359.4 pm.[31] Expanding the basis set from 6-31+G(d) to 6-311++G(d,p) improves the calculated geometries only marginally. Figure 3 shows the B3LYP/6-311++G(d,p)-optimized C_2-twisted conformations of **E11′F2**, **Z11′F2**, **E11′Cl2**, and **Z11′Cl2**. The principal mode of deviation from planarity of BFs is the twist angle ω around $C^9=C^{9'}$.[2] In the parent **BF**, ω = 32.0°,[8] while the

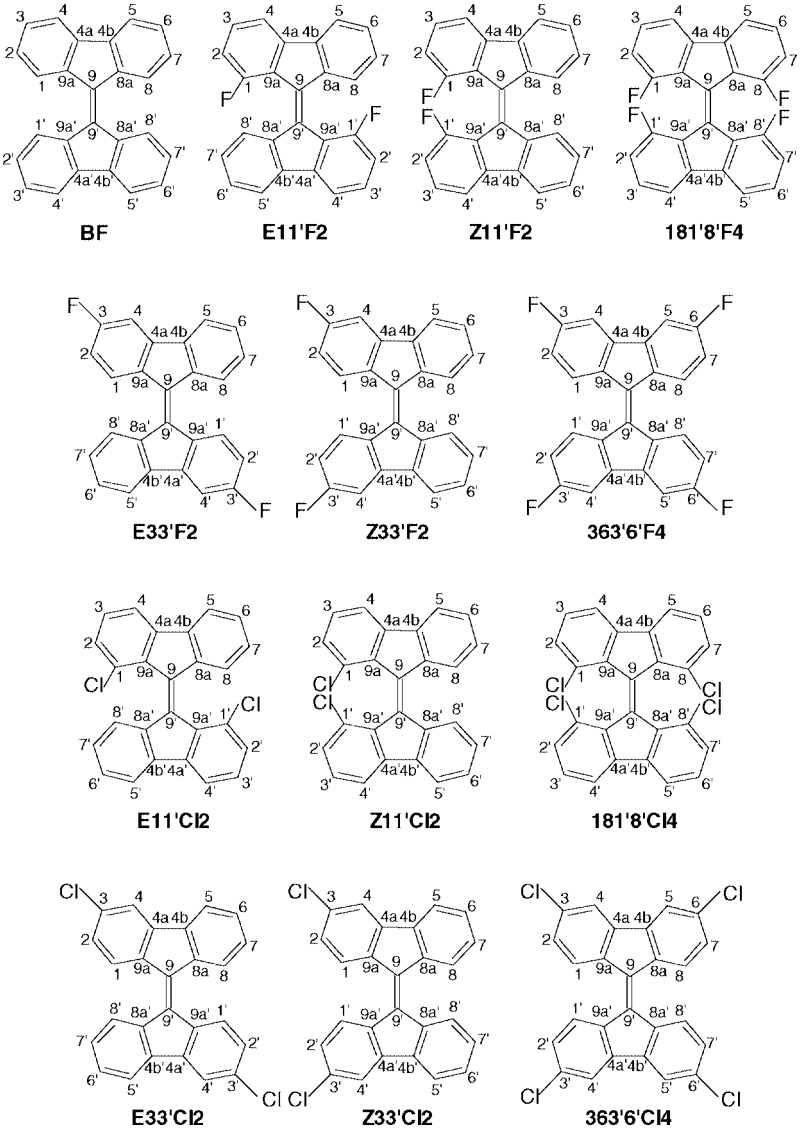

Figure 2. Substituted bifluorenylidenes.

Table 1. DFT-calculated relative energies, enthalpies and free energies [kJ/mol] of the various twisted substituted bifluorenylidenes.

		B3LYP/6-31G(d)			B3LYP/6-31+G(d)			B3LYP/6-311G(d,p)			B3LYP/6-311++G(d,p)		
		ΔE_{Tot}	ΔH_{298}	ΔG_{298}	ΔE_{Tot}	ΔH_{298}	ΔG_{298}	ΔE_{Tot}	ΔH_{298}	ΔG_{298}	ΔE_{Tot}	ΔH_{298}	ΔG_{298}
E11′F2	C_2	9.85	9.08	10.55	18.16	17.39	18.86	11.83	11.06	12.53	16.81	16.04	17.51
Z11′F2	C_2	6.05	5.46	7.66	16.06	15.47	17.67	9.07	8.48	10.68	14.75	14.15	16.36
E33′F2	C_2	0.00	0.00	0.00	0.00	0.00	0.00	0.00	0.00	0.00	0.00	0.00	0.00
Z33′F2	C_2	0.16	0.17	0.05	0.18	0.19	0.07	0.20	0.21	0.09	0.21	0.22	0.10
E11′Cl2	C_2	46.28	44.55	46.66	42.90	41.18	43.29	42.35	40.63	42.73	39.93	38.20	40.31
Z11′Cl2	C_2	48.63	46.83	49.15	45.47	43.67	45.99	44.83	43.03	45.35	42.21	40.41	42.73
E33′Cl2	C_2	0.00	0.00	0.00	0.00	0.00	0.00	0.00	0.00	0.00	0.00	0.00	0.00
Z33′Cl2	C_2	0.20	0.28	0.19	0.22	0.30	0.21	0.25	0.33	0.24	0.23	0.31	0.22
181′8′F4	D_2	10.44	9.40	13.94	29.77	28.74	33.27	16.15	15.11	19.65	27.16	26.12	30.66
363′6′F4	D_2	0.00	0.00	0.00	0.00	0.00	0.00	0.00	0.00	0.00	0.00	0.00	0.00
181′8′Cl4	D_2	92.95	89.74	93.69	86.34	83.13	87.08	85.64	82.44	86.39	80.35	77.14	81.09
363′6′Cl4	D_2	0.00	0.00	0.00	0.00	0.00	0.00	0.00	0.00	0.00	0.00	0.00	0.00

Table 2. DFT-calculated relative energies, enthalpies and free energies [kJ/mol] of a series of homodesmotic reactions of the various bifluorenylidenes.

#	Homodesmotic reaction	B3LYP/6-31G(d)			B3LYP/6-31+G(d)			B3LYP/6-311G(d,p)			B3LYP/6-311++G(d,p)		
		ΔE_{Tot}	ΔH_{298}	ΔG_{298}	ΔE_{Tot}	ΔH_{298}	ΔG_{298}	ΔE_{Tot}	ΔH_{298}	ΔG_{298}	ΔE_{Tot}	ΔH_{298}	ΔG_{298}
1	**E11′F2 + E11′F2 = 181′8′F4 + BF**	–7.11	–6.68	–1.97	–3.69	–3.26	1.45	–4.97	–4.54	0.17	–3.53	–3.11	1.61
2	**Z11′F2 + Z11′F2 = 181′8′F4 + BF**	0.49	0.57	3.82	0.50	0.58	3.84	0.54	0.62	3.88	0.58	0.66	3.92
3	**E33′F2 + E33′F2 = 363′6′F4 + BF**	2.15	2.08	5.20	2.86	2.79	5.91	2.54	2.47	5.59	2.92	2.85	5.97
4	**Z33′F2 + Z33′F2 = 363′6′F4 + BF**	1.82	1.74	5.09	2.50	2.42	5.77	2.14	2.05	5.41	2.50	2.42	5.77
5	**E11′Cl2 + E11′Cl2 = 181′8′Cl4 + BF**	4.29	4.42	7.32	4.04	4.17	7.07	4.94	5.07	7.97	3.63	3.77	6.67
6	**Z11′Cl2 + Z11′Cl2 = 181′8′Cl4 + BF**	–0.42	–0.12	2.35	–1.10	–0.80	1.67	–0.03	0.27	2.74	–0.94	–0.64	1.84
7	**E33′Cl2 + E33′Cl2 = 363′6′Cl4 + BF**	3.89	3.79	6.95	3.50	3.40	6.57	3.99	3.88	7.05	3.14	3.03	6.20
8	**Z33′Cl2 + Z33′Cl2 = 363′6′Cl4 + BF**	3.48	3.23	6.57	3.06	2.81	6.15	3.48	3.23	6.57	2.68	2.42	5.76
9	**2×E11′F2 + 363′6′F4 = 2×E33′F2 + 181′8′F4**	–9.26	–8.76	–7.17	–6.55	–6.05	–4.46	–7.50	–7.01	–5.42	–6.45	–5.95	–4.36
10	**2×Z11′F2 + 363′6′F4 = 2×Z33′F2 + 181′8′F4**	–1.34	–1.17	–1.27	–2.00	–1.83	–1.94	–1.59	–1.43	–1.53	–1.92	–1.75	–1.86
11	**2×E11′Cl2 + 363′6′Cl4 = 2×E33′Cl2 + 181′8′Cl4**	–3.90	–3.35	–4.22	–4.16	–3.61	–4.48	–3.51	–2.96	–3.83	–3.61	–3.06	–3.93
12	**2×Z11′Cl2 + 363′6′Cl4 = 2×Z33′Cl2 + 181′8′Cl4**	0.39	0.63	0.36	0.54	0.78	0.51	0.95	1.19	0.92	0.49	0.73	0.47

Table 3. Selected calculated [B3LYP/6-311++G(d,p)] and experimental geometrical parameters of the twisted conformations of substituted (X = F, Cl) bifluorenylidenes.

	ΔE_{Tot} [kJ/mol]	Pure twist [°]	Fold [°]	Dihedral twist [°]	$\chi(C^9)$[a] [°]	C^9–$C^{9'}$ [pm]	X–C [pm]	$C^1\cdots C^{8'}$ (*E*) $C^1\cdots C^{1'}$ (*Z*) [pm]	$X^1\cdots H^{8'}$ (*E*) $X^1\cdots X^{1'}$ (*E*) [pm]	$H^8\cdots H^{8'}$ [pm]	$X^1\cdots C^{8'}$ (*E*) $X^1\cdots C^{1'}$ (*Z*) [pm]	$C^1\cdots H^{8'}$ (*E*) $C^8\cdots H^{8'}$ (*Z*) [pm]
BF	–	34.0	2.6	42.7	0.0	137.8	–	321.2	225.8	225.8	–	259.9
E11′F2	16.81	37.1	3.7	48.0	7.0*s*	138.1	135.2	333.0	249.6	–	282.5	265.4
Z11′F2	14.75	37.1	2.8	46.1	1.0*a*	138.2	135.2	343.2	270.7	227.9	283.5	261.7
Z11′F2[b]	–	*37.8*	*5.0*	*49.4*	*0.8a*	*137.7*	*134.5*	*347.2*	*263.8*	*234.8*	*275.5*	*267.7*
E33′F2	0.00	34.0	2.7	42.7	0.2*s*	137.8	135.5	321.3	–	225.9	–	259.9
Z33′F2	0.21	33.9	2.6	42.6	0.4*a*	137.8	135.5	320.8	–	225.3	–	260.0
E11′Cl2	39.93	40.6	4.7	55.7	12.7*s*	138.4	175.4	342.8	292.6	–	322.6	270.5
Z11′Cl2	42.21	42.7	3.6	51.9	2.0*a*	138.6	175.4	375.3	358.3	235.0	331.0	263.8
Z11′Cl2[b]	–	*40.4*	*4.0, 2.6*	*49.7*	*1.9a, 1.7a*	*137.9*	*172.5, 172.7*	*370.5*	*359.4*	*253.0*	*321.5, 321.8*	*259.0, 277.7*
E33′Cl2	0.00	34.1	2.6	42.8	0.4*s*	137.8	175.8	321.5	–	226.1	–	260.6
Z33Cl2	0.23	34.0	2.5	42.6	0.1*a*	137.8	175.8	320.9	–	225.4	–	260.1
181′8′F4	27.16	40.3	1.9	49.6	0.0	138.7	135.1	344.9	271.9	–	285.1	–
363′6′F4	0.00	33.8	2.5	42.5	0.0	137.8	135.4	321.1	–	226.4	–	260.2
181′8′Cl4	80.35	52.6	1.7	61.8	0.0	139.9	175.3	378.7	366.4	–	336.8	–
13681′3′6′8′Cl8[b]	–	*55*	*2.9, 3.8*	*2.0,2.5 2.6,2.7*	*2.8, 1.7*	*139.2*	*173.1, 172.9, 173.4, 173.8*	*137.4, 138.2*	*365.6, 355.8*	–	*336.4, 331.0, 332.7, 336.4*	–
363′6′Cl4	0.00	33.9	2.4	42.5	0.0	137.9	175.6	321.4	–	226.7	–	260.6

[a] *s* and *a* designate *syn*- and *anti*-pyramidalization, respectively. [b] The geometrical parameters taken from the X-ray molecular structures.

fluorenylidene moieties are almost planar (folding dihedral angle: 5.2–2.7°).[2] Introduction of fluorine or chlorine substituents at positions 3, 6, 3′ and 6′ hardly affects the twist. For example, in **363′6′F4** and **363′6′Cl4** ω = 33.8° and 33.9°, respectively. These results indicate that the degree of overcrowding in BF is maintained in these derivatives. A different picture emerges when fluorine or chlorine substituents are introduced in the *fjord* regions: the degree of twist is enhanced. In **E11′F2** and **Z11′F2**, ω = 37.1°. As expected, introduction of chlorine substituents results in a larger twist angle. For example, in **181′8′F4**, ω = 40.3°, while in **181′8′Cl4**, ω = 52.6°. For comparison, in **13681′3′6′8′Cl8** and in perchlorobifluorenylidene, ω = 55° and 66°, respectively.[26] Surprisingly, the two diastereomers **E11′F2** and **Z11′F2** have identical twists, ω = 37.1°. By contrast, in **E11′Cl2** and **Z11′Cl2**, ω = 40.6° and 42.7°, respectively. At first glance, it seems that there is no difference in the degree of overcrowding in the *fjord* regions of **E11′F2** and **Z11′F2**. However, these (*E*) and (*Z*) diastereomers differ in the degree and mode of pyramidalization, χ, at C^9 and $C^{9'}$. In **E11′F2**, $\chi(C^9) = +\chi(C^{9'}) = 7.0°$ (*syn*-pyramidalization), while in **Z11′F2**, $\chi(C^9) = -\chi(C^{9'}) = 1.0°$ (*anti*-pyramidalization). The *syn*-pyramidalization of the (*E*) diastereomer and the *anti*-pyramidalization of the (*Z*) diastereomer are dictated by the orientation of the two-fold C_2 axis relative to $C^9{=}C^{9'}$, which passes through the center of the double bond perpendicularly to the mean plane of the molecule [(*E*) diastereomer] and through the center of the *fjord* region [(*Z*) diastereomer]. From this point of view, the (*E*) diastereomer is more overcrowded than the (*Z*) diastereomer. The higher stability of **Z11′F2** relative to **E11′F2** may be attributed to the difference in the degree and sign of the pyramidalization at C^9 and $C^{9'}$. In **181′8′F4**, with two pairs of bucking fluorine atoms in the *fjord* regions [(*Z*) to one another], D_2 symmetry dictates that $\chi(C^9) = \chi(C^{9'}) = 0°$. In this case, the burden of overcrowding falls on the twist angle: ω = 40.3°. In **E11′Cl2**, the pyramidalization of C^9 is considerably higher than in **E11′F2**, $\chi(C^9) = 12.7°$ (*syn*), while in **Z11′Cl2**, the pyramidalization of C^9 is still very small, $\chi(C^9) = 2.0°$ (*anti*), similar to that in **Z11′F2**. Another indication of overcrowding in the *fjord* regions is the penetration across the *fjords*, when the nonbonding interatomic distance of the relevant pair of atoms is smaller than their van der Waals contact distances. The van der Waals radii of hydrogen, fluorine, carbon and chlorine are 115 pm (H), 140 pm (F), 171 pm (C) and 190 pm (Cl).[32] Therefore, the van der Waals contact distances are 280 (F···F), 380 (Cl···Cl), 342 (C···C), 230 (H···H), 255 (F···H), 305 (Cl···H), 311 (F···C), 361 (Cl···C), and 286 (C···H) pm. Only slight penetration (ca. 8%) across the *fjord* regions has mostly been observed. The highest degrees of penetration are found between the *fjord* region carbon atoms and the opposite substituents. The C···H distances in the parent compound (**BF**) and in the 3,3′-disubstituted derivatives (**E33′F2**, **Z33′F2**, **E33′Cl2**, and **Z33′Cl2**) are 260–261 pm, corresponding to 9% penetration. The C···F distances in **E11′F2**, **Z11′F2**, and **181′8′F4** range from 283 to 285 pm, corresponding to 8–9% penetra-

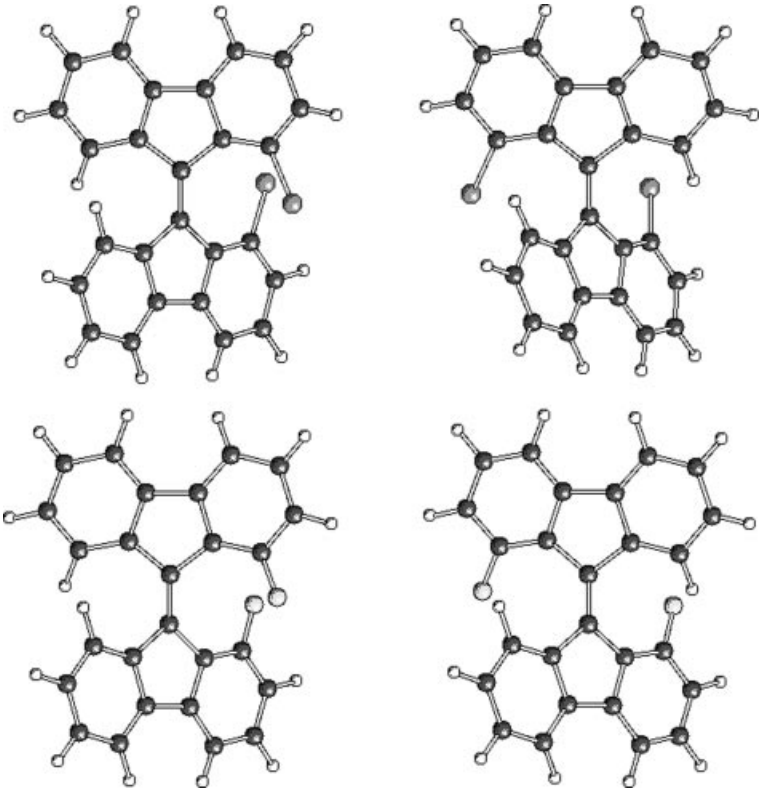

Figure 3. Optimized C_2-twisted conformations of **Z11′Cl2** (top left), **E11′Cl2** (top right), **Z11′F2** (bottom left) and **E11′F2** (bottom right) [at B3LYP/6-311++G(d,p)].

tion. The C···Cl distances are 323 pm (11% penetration) in **E11′Cl2**, 331 pm (8% penetration) in **Z11′Cl2** and 337 pm (7% penetration) in **363′6′Cl4**. All other nonbonding distances across the *fjord* regions correspond to penetrations of 6% or less.

Energies

The energies presented in Table 1 are calculated with the 6-311++G(d,p) basis set. In order to obtain more reliable energies of noncovalent interactions, the basis set should contain polarization and diffuse functions.[33] The data presented in Table 1 show the importance of including the diffuse function on carbon atoms. Omitting them overestimates by a factor of two the stability of **E11′F2** and **Z11′F2** relative to **E33′F2**, and slightly underestimates the stability of **E11′Cl2** and **Z11′Cl2** relative to **E33′Cl2**. On the other hand, expanding the basis set from 6-31+G(d) to 6-311++G(d,p) hardly affects the results. Addition of polarization and diffuse functions to hydrogen atoms slightly stabilizes 1,8-disubstituted BFs relatively to 3,6-disubstituted ones. Table 1 also gives the relative enthalpies, ΔH_{298}, and the relative free energies, ΔG_{298}, calculated from thermal corrections computed at the B3LYP/6-31G(d) level.

E33′F2 and **Z33′F2** have essentially equal relative energies. The same is true for **E33′Cl2** and **Z33′Cl2**. Overcrowded **E11′F2** and **Z11′F2** are significantly less stable than **E33′F2** and **Z33′F2**: ΔH_{298} = 16.0 and 13.9 kJ/mol, respectively. **E11′Cl2** and **Z11′Cl2** are considerably less stable than **E33′Cl2** and **Z33′Cl2**: ΔH_{298} = 38.2 and 40.1 kJ/mol, respectively. Thus, introduction of fluorine or chlorine substituents in the *fjord* regions leads to destabilization, both in the (*E*) diastereomer and in the (*Z*) diastereomer. The destabilizing effect of halogen substitution in a *fjord* region is approximately doubled for tetrahalogenated compounds: **181′8′F4** is less stable than **363′6′F4** by 26.1 kJ/mol, while **181′8′Cl4** is higher in energy than **363′6′Cl4** by 77.1 kJ/mol (ΔH_{298}).

Surprisingly, in the fluorine series, **Z11′F2** is more stable than **E11′F2**: ΔH_{298} = –1.9 kJ/mol, ΔG_{298} = –1.2 kJ/mol, contrary to the expectation that bucking fluorine atoms and hydrogen atoms across the *fjord* regions of the (*Z*) diastereomer would be sterically more demanding than a pair of bucking fluorine and hydrogen atoms in the *fjord* regions of the (*E*) diastereomer.[25] This result is consistent with the experimental ratio (*Z*)/(*E*) = 69:31 (2.2:1, ΔG_{298} = –2.0 kJ/mol) observed in the ^{1}H NMR spectrum of a mixture of **Z11′F2** and **E11′F2** in solution.[24]

In the chlorine series, the (*Z*)/(*E*) ratio is reversed: **Z11′Cl2** is less stable than **E11′Cl2**: ΔH_{298} = 2.2 kJ/mol, ΔG_{298} = 2.4 kJ/mol. Bucking chlorine atoms and bucking hydrogen atoms in the *fjord* regions of the (*Z*) diastereomer are indeed sterically more demanding than a pair of bucking chlorine and hydrogen atoms in the *fjord* regions of the (*E*) diastereomer. This result is also consistent with the experimental ratio of (*Z*)/(*E*) = 30:70 (1:2.3, ΔG_{298} = 2.1 kJ/mol) observed in the ^{1}H NMR spectrum of a mixture of **Z11′Cl2** and **E11′Cl2** in solution.[31]

The unexpected relative stability of the (*Z*) stereochemistry of fluorine atoms in a *fjord* region of BFs is reflected also in a series of homodesmotic reactions[34] (Table 2). In particular, in the fluorine series, (*Z*)-difluoro-BFs have a stability comparable to the average of the 1,8,1′,8′-tetrachloro-**BF** and the parent **BF** (and the pure twist angle, 37.1°, comparable to the average pure twist angles of **181′8′F4**, 40.3°, and **BF**, 34.0°): ΔH_{298} = +0.7 kJ/mol for **Z11′F2** + **Z11′F2** → **181′8′F4** + **BF**, while for **E11′F2** + **E11′F2** → **181′8′F4** + **BF**, ΔH_{298} = –3.1 kJ/mol. By contrast, in the chlorine series, ΔH_{298} = +3.8 kJ/mol for **E11′Cl2** + **E11′Cl2** → **181′8′Cl4** + **BF** and ΔH_{298} = –0.6 kJ/mol for **Z11′Cl2** + **Z11′Cl2** → **181′8′Cl4** + **BF**. In the latter case, the steric strain in **181′8′Cl4** is reduced due to its significantly larger twist angle, 52.6° vs. 42.7° in **Z11′Cl2**. In the 3,6-disubstituted series, the average stability of each of the tetrasubstituted BFs and **BF** is less than the stability of the respective disubstituted BF (Table 2).

In general, the relative enthalpies of 1,1′-disubstituted and 1,8,1′,8′-tetrasubstituted BFs are lower than the respective relative energies by 0.6–3.2 kJ/mol, while the entropy effect manifests itself in the destabilization of 1,8-disubstituted BFs by 1.5–4.5 kJ/mol.

Electronic Structure

The natural atomic charges [at the B3LYP/6-311++G(d,p) level] of the BFs under study are provided in Table S3. The C–F bond has a significant ionic character in both **E11′F2** and **Z11′F2**, as demonstrated by the high charges on the F^1 (–0.343 and –0.345, respectively) and C^1 (0.436 and 0.450, respectively) atoms. The carbon–fluorine bonds in **E33′F2** and **Z33′F2** are similarly polarized. By contrast, the carbon–chlorine bonds in **E11′Cl2** and **Z11′Cl2** are nearly purely covalent, with Cl^1 charged slightly positive (0.028 and 0.023, respectively) and C^1 bearing a small charge (–0.013 and 0.016, respectively). According to the natural bond orbital (NBO) analysis of the C^1–F^1 and C^1–Cl^1 bonds, the natural atomic hybrid on chlorine has notably higher p character, $sp^{4.68}d^{0.03}$, than the analogous hybrid on fluorine, $sp^{2.31}$ [(*E*) diastereomers]. The high p component in the spd hybrid (in the direction of the bond) is due to the fact that a 3s orbital of Cl is too diffuse for a good overlap with the sp^2 hybrid (2s,2p) of the carbon atom aligned along the bond.

The C$^{8'}$–H$^{8'}$ and C^8–H^8 bonds of **E11′F2** and **Z11′F2**, respectively, are also polar, with negatively charged carbon atoms and positive hydrogen atoms. Taking into consideration only the C–F and C–H bonds of the *fjord* regions of **E11′F2** and **Z11′F2**, two different point charge models, so called "ion triplets",[35] were examined, as depicted in Figure 4.

Considering Coulomb's law, the net electrostatic energy of the collection of charges corresponding to **Z11′F2** (Figure 4) would be given by Equation (1).

The analogous expression for the net electrostatic energy of model describing **E11′F2** is given by Equation (2).

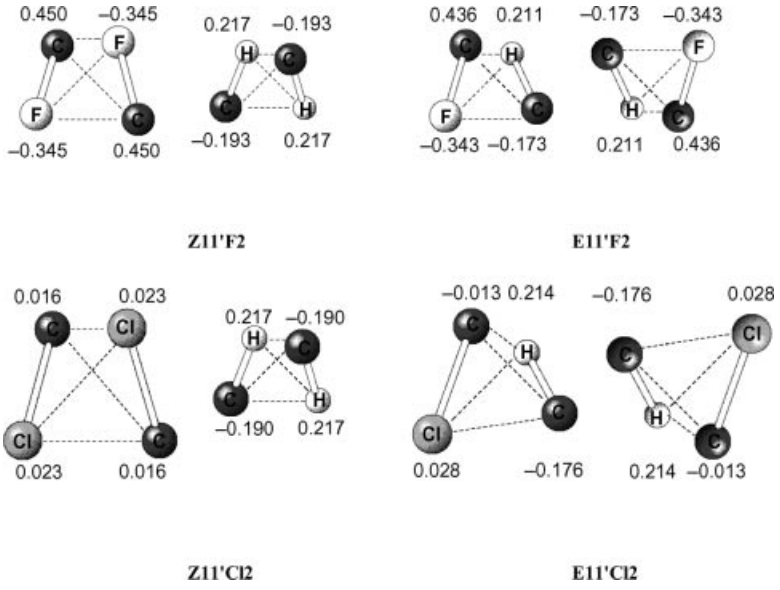

Figure 4. Point charge models of the *fjord* regions of 1,8′-dihalobifluorenylidenes together with natural atomic charges [at the B3LYP/6-311++G(d,p) level].

$$E^{C}_{(\mathbf{Z11'F2})} = 2q_{C^1}q_{F^1}r_{(C^1\cdots F^1)}^{-1} + q_{F^1}q_{F^{1'}}r_{(F^1\cdots F^{1'})}^{-1} + 2q_{C^1}q_{F^{1'}}r_{(C^1\cdots F^{1'})}^{-1} + q_{C^1}q_{C^{1'}}r_{(C^1\cdots C^{1'})}^{-1} + 2q_{C^8}q_{H^8}r_{(C^8-H^8)}^{-1} + 2q_{C^8}q_{H^{8'}}r_{(C^8\cdots H^{8'})}^{-1} + q_{C^8}q_{C^{8'}}r_{(C^8\cdots C^{8'})}^{-1} + q_{H^8}q_{H^{8'}}r_{(H^8\cdots H^{8'})}^{-1} \quad (1)$$

$$E^{C}_{(\mathbf{E11'F2})} = 2[q_{C^1}q_{F^1}r_{(C^1-F^1)}^{-1} + q_{C^{8'}}q_{H^{8'}}r_{(C^{8'}-H^{8'})}^{-1} + q_{C^1}q_{H^{8'}}r_{(C^1\cdots H^{8'})}^{-1} + q_{C^1}q_{C^{8'}}r_{(C^1\cdots C^{8'})}^{-1} + q_{F^1}q_{H^{8'}}r_{(F^1\cdots H^{8'})}^{-1} + q_{F^1}q_{C^{8'}}r_{(F^1\cdots C^{8'})}^{-1}] \quad (2)$$

At the 6-311++G(d,p) level, $E^{C}_{(\mathbf{E11'F2})}$ = –390.1 kJ/mol, while $E^{C}_{(\mathbf{Z11'F2})}$ = –435.6 kJ/mol, with the energy difference ΔE^{C} = –45.5 kJ/mol in favour of **Z11′F2**. For comparison, the net electrostatic energy calculated for the two pairs of C–H bonds in the *fjord* region of the parent **BF** is –106.7 kJ/mol. From examining the separate terms in Equations (1) and (2), it follows that the energy losses in **Z11′F2** because of the repulsive $F^1\cdots F^{1'}$ (61.2 kJ/mol) and $C^1\cdots C^{1'}$ (81.9) interactions are outweighed by the energy gain due to the two attractive $C^1\cdots F^{1'}$ (–152.2) and $C^8\cdots H^{8'}$ (–44.5) interactions. Thus, considering only Coulomb interactions, the (*Z*) diastereomer is considerably stabilized relative to the (*E*) diastereomer. In the case of **E11′Cl2** and **Z11′Cl2**, the difference is much smaller, with $E^{C}_{(\mathbf{E11'Cl2})}$ = –96.8, $E^{C}_{(\mathbf{Z11'Cl2})}$ = –105.0, and ΔE^{C} = –8.2 kJ/mol. Note that introduction of two fluorine atoms into the *fjord* regions of **BF** leads to stabilizing Coulomb interaction as compared to the parent **BF**, whereas **E11′Cl2** and **Z11′Cl2** are considerably less stabilized due to the presence of two chlorine atoms.

Alternatively, the charge distributions depicted in Figure 4 can be described as constructed of dipoles $C^{\delta+}$–$F^{\delta-}$ and $C^{\delta-}$–$H^{\delta+}$ rather than of point charges. The charge models are then reduced to the two pairs of dipoles, which experience dipole–dipole interactions depending on r^{-3}[36] [Equation (3)], where $\mu_{(C^1-F^1)}$ and $\mu_{(C^{8'}-H^{8'})}$ are the dipole moment vectors of the respective isolated bonds, and **R** is the vector joining this two bonds.

$$E^{d-d}_{(\mathbf{E11'F2})} = 2[\mu_{(C^1-F^1)}\mu_{(C^{8'}-H^{8'})}\mathbf{R}_{(C^1-F^1\cdots C^{8'}-H^{8'})}^{-3} - 3(\mu_{(C^1-F^1)}R_{(C^1-F^1\cdots C^{8'}-H^{8'})})(\mu_{(C^{8'}-H^{8'})}R_{(C^1-F^1\cdots C^{8'}-H^{8'})})\mathbf{R}_{(C^1-F^1\cdots C^{8'}-H^{8'})}^{-5}] \quad (3)$$

The dipole–dipole interaction energy for the **Z11′F2** model would be written as Equation (4).

$$E^{d-d}_{(\mathbf{Z11'F2})} = \mu_{(C^1-F^1)}\mu_{(C^{1'}-F^{1'})}\mathbf{R}_{(C^1-F^1\cdots C^{1'}-F^{1'})}^{-3} - 3(\mu_{(C^1-F^1)}R_{(C^1-F^1\cdots C^{1'}-F^{1'})})(\mu_{(C^{1'}-F^{1'})}R_{(C^1-F^1\cdots C^{1'}-F^{1'})})\mathbf{R}_{(C^1-F^1\cdots C^{1'}-F^{1'})}^{-5} + \mu_{(C^8-H^8)}\mu_{(C^{8'}-H^{8'})}\mathbf{R}_{(C^8-H^8\cdots C^{8'}-H^{8'})}^{-3} - 3(\mu_{(C^8-H^8)}R_{(C^8-H^8\cdots C^{8'}-H^{8'})})(\mu_{(C^{8'}-H^{8'})}R_{(C^8-H^8\cdots C^{8'}-H^{8'})})\mathbf{R}_{(C^8-H^8\cdots C^{8'}-H^{8'})}^{-5} \quad (4)$$

The dipole moments for C–F bonds in **E11′F2** and **Z11′F2**, calculated from the bond lengths and natural atomic charges,[37] are 2.59 and 2.65 D, respectively, and the dipole moments for $C^{8'}$–$H^{8'}$ (**E11′F2**) and C^8–H^8 (**Z11′F2**) are 1.07 and 1.11 D, respectively. Hence, the dipole–dipole interaction energies for **E11′F2** and **Z11′F2** (Figure 4) are $E^{d-d}_{(\mathbf{E11'F2})}$ = 10.9 and $E^{d-d}_{(\mathbf{Z11'F2})}$ = 17.3 kJ/mol, respectively. The resulting ΔE^{d-d} = 6.4 kJ/mol shows modest destabilization of the (*Z*) diastereomer as compared to the (*E*) diastereomer. Similarly, **Z11′Cl2** (E^{d-d} = 3.4 kJ/mol) is destabilized by the dipole–dipole interaction energies relative to **E11′Cl2** (E^{d-d} = 0.5 kJ/mol).

Although the electrostatic energies derived from the sole collection of charges presented in Figure 4 are approximate, they nevertheless give a good insight into noncovalent interactions in halogen-substituted BFs.

Relative Stability of (*E*) vs. (*Z*) Diastereomers

As noted previously, **Z11′F2** is more stable than **E11′F2** (ΔH_{298} = –1.9 kJ/mol, ΔG_{298} = –1.2 kJ/mol), while **Z11′Cl2** is less stable than **E11′Cl2** (ΔH_{298} = 2.2 kJ/mol, ΔG_{298} = 2.4 kJ/mol). The stability difference can be explained by a

combination of steric and electronic effects. In the fluorine series, the degree of overcrowding in the *fjord* region of **E11′F2** and **Z11′F2** is comparable, with identical twist angles (ω = 37.1°) and close dihedral *AEB–CFD* angles (48.0° and 46.1°, respectively) and nonbonding C···F distances (282.5 and 283.5, respectively). The contact $F^1 \cdots F^{1'}$ distance in **Z11′F2** is 271.0 pm (3% penetration), and the dipole–dipole interaction between fluorine atoms corresponds to the nonstabilizing type I (angle $C^1–F^1 \cdots F^{1'}$ 81.2°).[38] **E11′F2** is still more overcrowded as reflected by the higher pyramidalization, $\chi(C^9)$ = 7.0° vs. 1.0°. In a similar fashion, **E11′Cl2** is sterically more strained as compared to **Z11′Cl2**, considering smaller pure twist angle (ω = 40.6° vs. 42.7°) but shorter C···Cl distance (322.6 vs. 331.0) and higher pyramidalization $\chi(C^9)$ = 12.7° vs. 2.0°.

The preference of **Z11′F2** may be compared to the higher stabilities of most (*Z*)-1,2-dihaloethylenes relative to their (*E*) diastereomers, termed the *cis* effect, ascribed usually to nonbonding interactions between halogen atoms.[39] Thus, for (*E*)/(*Z*) isomerization of 1,2-difluoroethylene, $\Delta H°$ = 3.88 kJ/mol,[40] and the evaluated electronic energy differences is 4.52 kJ/mol,[41] with the (*Z*) diastereomer having the lower energy. According to the NBO-based second-order perturbation-theory analysis of electron delocalization in (*Z*)-1,2-difluoroethylene,[42,43] geminal, vicinal stabilizing interaction of C–F bonds and lone-pair interactions of the fluorine lone-pair electrons are considered, with the latter being the most important. Indeed, the delocalization energy of the fluorine lone pairs in **E11′F2** and **Z11′F2** are 92.6 and 94.5 kJ/mol [at the B3LYP/6-31+G(d) level], respectively, with the energy difference of 1.9 kJ/mol being mostly due to $n_\sigma^F \rightarrow \pi_{CC}^*$ excitations. At the B3LYP/6-311++G(d,p) level, however, the delocalization energies of **E11′F2** and **Z11′F2** are 85.5 and 84.9 kJ/mol, respectively.

The Coulomb interactions in the *fjord* regions were demonstrated to increase the stability of **Z11′F2** relative to **E11′F2** by –45.5 kJ/mol, while the stabilization of **Z11′Cl2** is only –8.2 kJ/mol. Finally, taking into account dipole–dipole interactions including C–X and C–H bonds, both (*Z*) diastereomers are destabilized relative to the (*E*) diastereomers by 2.9–6.4 kJ/mol. Thus, both geometric and energetic effect account for the relative stability of **Z11′F2** and **E11′Cl2** over their respective diastereomers.

Through-Space Interactions in Z11′F2

Because of the symmetry of the molecule, the two fluorine atoms in **Z11′F2** have the same chemical shift. The same is true for the diastereomer **E11′F2**. However, in the ^{13}C isotopomers, $^{13}C–^{19}F–^{19}F–^{12}C$, the two fluorine atoms have different chemical shifts due to an isotope effect, and any measurable coupling between them is easily observed as a splitting of the ^{13}C satellites of the main fluorine resonances. The ^{19}F spectra are especially simple when recorded with complete ^1H decoupling, which removes the complexity that would otherwise be caused by $^{19}F–^1H$ coupling.

The following results were obtained; for **E11′F2**: $\delta(^{19}F–^{12}C)$ = 118.74 ppm, $\delta(^{19}F–^{13}C)$ = 118.83 ppm, $^1J_{C–F}$ = 246.3 Hz; for **Z11′F2**: $\delta(^{19}F–^{12}C)$ = 119.71 ppm, $\delta(^{19}F–^{13}C)$ = 119.80 ppm, $^1J_{C–F}$ = 262.3 Hz, $^7J_{F–F}$ = 11.0 ± 0.4 Hz, $^6J_{C–F}$ = 4.8 Hz.

No splitting was observed in the ^{13}C satellites of the ^{19}F resonance in the spectrum of **E11′F2**, which is perhaps not unexpected, given the separation of its two fluorine atoms. The corresponding resonances of **Z11′F2** show splittings of 11.0 ± 0.4 Hz and 4.8 Hz, which are ascribed to long-range fluorine–fluorine and fluorine–carbon coupling across the *fjord*, respectively.

Kresmar et al.,[24] on the basis of analysis of the ^1H NMR spectrum, reported 11.0 Hz for the $^7J_{F–F}$ coupling, but did not report the details of the ^{19}F spectrum. The ^{13}C data differ slightly from ours, with Kresmar reporting $^1J_{C–F}$ = 260.2 Hz for **E11′F2** and 265.2 or 255.5 Hz for **Z11′F2**, compared to our value of 262.3 Hz. However, the $^7J_{F–F}$ values are similar: 11.0 vs. our 11.4 Hz. The authors comment that the value for this coupling constant "is rather small in relation to the value of ca. 46 Hz" that they predict from use of an empirical equation relating the F–F distance with the size of the spin–spin coupling interaction. However, this equation was devised to correlate data from a series of [2.2]-metacyclophanes, in which the C–F bonds are substantially parallel, rather than antiparallel in the case of the bifluorenylidenes. Thus, the correlation seems to have limited value outside the domain for which it was devised.

The long-range couplings in the bifluorenylidenes would be much larger if the molecular framework were planar or close to planar, but would be expected to fall off rapidly as the fluorine–fluorine distance increases. Preliminary calculations[44] suggest that both the $^7J_{F–F}$ couplings would decrease sharply as the twist angle around the central C=C bond increased from 40° to 50° (from 250 to 19 Hz), but these calculations did not take into account the concomitant pyramidalization, and, while the trend is no doubt correct, the calculated values are high.

Because no system exists for correlation of the magnitude of through-space coupling with the disposition of the fluorine atoms and their respective C–F bonds, it is not possible to make deductions about the structures on the basis of the $J_{F–F}$ values, except to say that these are consistent with the fluorine atoms in **Z11′F2** being close to each other.

Conclusions

The (*Z*) diastereomers **Z11′F2** and **Z11′Cl2** were found to be overcrowded, in a similar degree, relative to their respective (*E*) diastereomers. The higher steric strain in **E11′F2** and **E11′Cl2** is reflected in their pyramidalization at C^9 and $C^{9'}$. **Z11′F2** is more stable than **E11′F2** by 1.2 kJ/mol, whereas **Z11′Cl2** is less stable than **E11′Cl2** by 2.4 kJ/mol. This difference in stability can be explained by a combination of steric factors, electrostatic Coulombic and dipole–dipole interactions. The ^{19}F NMR spectrum of

Z11′F2 shows long-range fluorine–fluorine and carbon–carbon coupling across the *fjord* region.

Experimental Section

Calculations: The DFT calculations of bifluorenylidenes were performed using the Gaussian03[45] package. Becke's three-parameter hybrid density functional B3LYP,[46] with the nonlocal correlation functional of Lee, Yang, and Parr[47] was used. The basis sets 6-31G(d), 6-31+G(d), 6-311G(d,p) and 6-311++G(d,p) were employed. All structures were fully optimized using symmetry constraints as indicated. Vibrational frequencies were calculated to verify minima at the B3LYP/6-31G(d) level. Nonscaled thermal energy corrections calculated at the B3LYP/6-31G(d) level were used. Natural bond orbital (NBO) analysis[48] was performed by the NBO version 3.0 module as a part of Gaussian03 program.

NMR Spectroscopy: The ^{19}F NMR spectra were measured at 282.41 MHz with a Bruker AM3000 spectrometer, for dilute solutions of **E11′F2** and **Z11′F2** in $CDCl_3$ at room temperature with $CFCl_3$ as internal standard. The digital resolution was 0.09 Hz/point, and ^1H decoupling was complete. The mixture of (*E*) and (*Z*) diastereomers was purified by chromatography (benzene/alumina) shortly before the NMR spectra were recorded. The ratio varied across the fractions collected from the column, suggesting different chromatographic mobilities for the two diastereomers. The ^{19}F NMR spectra reported here were recorded for a mixture of (*Z*)/(*E*) = 3:1.

Supporting Information (see also footnote on the first page of this article): DFT total energies, enthalpies, and free energies, additional geometrical parameters, natural atomic charges and Mulliken atomic charges of bifluorenylidenes under study.

Acknowledgments

I. D. R. acknowledges the assistance of Dr. J. A. Weigold (Monash University) in obtaining the NMR spectra, and of Professor Ruben Contreras (Departamento de Fisica, Universidad de Buenos Aires) who performed preliminary calculations on the difluorobifluorenylidenes. We thank Dr. P. U. Biedermann (Max-Planck-Institut für Eisenforschung GmbH, Düsseldorf) for very helpful discussions and enlightening suggestions.

[1] G. Shoham, S. Cohen, R. M. Suissa, I. Agranat, in: *Molecular Structure: Chemical Reactivity and Biological Activity* (Eds.: J. J. Stezowski, J.-L. Huang, M.-C. Shao), IUCr Crystallographic Symposia 2, Oxford University Press, Oxford, **1988**, pp. 290–312.
[2] P. U. Biedermann, J. J. Stezowski, I. Agranat, in: *Advances in Theoretically Interesting Molecules* (Ed.: R. P. Thummel), JAI Press, Stanford, CN, **1988**, vol. 4, pp. 245–322.
[3] P. U. Biedermann, J. J. Stezowski, I. Agranat, *Chem. Eur. J.* **2006**, *12*, 3345–3354.
[4] P. U. Biedermann, J. J. Stezowski, I. Agranat, *Eur. J. Org. Chem.* **2001**, 15–34.
[5] P. U. Biedermann, A. Levy, J. J. Stezowski, I. Agranat, *Chirality* **1995**, *7*, 199–205.
[6] B. L. Feringa, *Acc. Chem. Res.* **2001**, *34*, 504–513.
[7] N. A. Bailey, S. E. Hull, *Acta Crystallogr., Sect. B* **1978**, *34*, 3289–3295.
[8] J.-S. Lee, S. C. Nyburg, *Acta Crystallogr., Sect. C* **1985**, *41*, 560–567.
[9] P. U. Biedermann, A. Levy, M. R. Suissa, J. J. Stezowski, I. Agranat, *Enantiomer* **1996**, *1*, 75–80.
[10] S. Pogodin, P. U. Biedermann, I. Agranat, in: *Recent Advances in the Chemistry of Fullerenes and Related Materials*, vol. 6 (Eds.: K. M. Kadish, R. S. Ruoff), The Electrochemical Society, Pennington, NJ, **1998**, pp. 1110–1116.
[11] H. E. Bronstein, N. Choi, L. T. Scott, *J. Am. Chem. Soc.* **2002**, *124*, 8870–8875.
[12] E. D. Bergmann, *Isomerism and Isomerization of Organic Compounds*, Interscience Publishers, New York, **1948**, p. 48.
[13] I. Gutman, S. J. Cyvin *Introduction to the Theory of Benzenoid Hydrocarbons*, Springer-Verlag, Berlin, **1989**, pp. 20–25.
[14] A. T. Balaban, M. Randić, *New J. Chem.* **2004**, *28*, 800–806.
[15] L. Peng, L. T. Scott, *J. Am. Chem. Soc.* **2005**, *127*, 16518–16521.
[16] S. Pogodin, I. Agranat, *J. Org. Chem.* **2002**, *67*, 265–270.
[17] P. G. Wislocki, A. Y. H. Luh, in: *Polycyclic Aromatic Hydrocarbon Carcinogenesis: Structure-Activity Relationships* (Eds.: S. K. Yang, B. D. Silverman), CRC Press, Boca Raton, FL, **1988**, pp. 1–27.
[18] A. K. Katz, H. L. Carrell, J. P. Glusker, *Carcinogenesis* **1998**, *19*, 1641–1648.
[19] S. L. Ralston, S. L. Coffing, A. Seidel, A. Luch, K.-L. Platt, W. M. Baird, *Chem. Res. Toxicol.* **1997**, *10*, 687–693.
[20] J. Jacob, *Pure Appl. Chem.* **1996**, *68*, 301–308.
[21] E. L. Cavalieri, E. G. Rogan, S. Higginbotham, P. Cremonesi, S. Salmasi, *J. Cancer Res. Clin. Oncol.* **1989**, *115*, 67–72.
[22] J. Iball, S. N. Scrimgeour, D. W. Young, *Acta Crystallogr., Sect. B* **1976**, *32*, 328–330.
[23] M. R. Osborn, N. T. Crosby *Benzopyrenes*; Cambridge University Press, Cambridge, **1987**.
[24] L. Kresmar, J. Grunenberg, I. Dix, P. G. Jones, K. Ibrom, L. Ernst, *Eur. J. Org. Chem.* **2005**, 5306–5312.
[25] I. Agranat, M. Rabinovitz, I. Gosnay, A. Weitzen-Dagan, *J. Am. Chem. Soc.* **1972**, *94*, 2889–2891.
[26] E. Molins, C. Miravitlles, E. Espinosa, M. Ballester, *J. Org. Chem.* **2002**, *67*, 7175–7178.
[27] F. De Proft, P. Geerlings, *Chem. Rev.* **2001**, *101*, 1451–1464.
[28] P. U. Biedermann, J. J. Stezowsky, I. Agranat, *Chem. Commun.* **2001**, 954–955.
[29] A. P. Scott, I. Agranat, P. U. Biedermann, N. V. Riggs, L. Radom, *J. Org. Chem.* **1997**, *62*, 2026–2038.
[30] I. Gosnay, E. D. Bergmann, M. Rabinovitz, I. Agranat, *Isr. J. Chem.* **1972**, *10*, 423–437.
[31] S. Pogodin, S. Cohen, P. U. Biedermann, I. Agranat, *Enantiomer* **2002**, *7*, 261–270.
[32] Y. V. Zefirov, *Crystallogr. Rep.* **1997**, *42*, 111–116.
[33] K. Müller-Dethlefs, P. Hobza, *Chem. Rev.* **2000**, *100*, 143–167.
[34] P. George, M. Trachtman, C. W. Bock, A. M. Brett, *Theor. Chim. Acta* **1975**, *38*, 121–129.
[35] A. Streitwieser Jr, *Acc. Chem. Res.* **1984**, *17*, 353–357.
[36] D. P. Craig, D. P. Mellor, *Top. Curr. Chem.* **1976**, *63*, 1–48.
[37] R. F. W. Bader, *An Introduction to the Electronic Structure of Atoms and Molecules*, Clarke, Irwin & Co. Ltd., Toronto, **1970**.
[38] K. Reichenbächer, H. I. Süss, J. Hulliger, *Chem. Soc. Rev.* **2005**, *34*, 22–30.
[39] R. Kanakaraju, K. Senthilkumar, P. Kolandaivel, *J. Mol. Struct. (Theochem)* **2002**, *589–590*, 95–102.
[40] N. C. Craig, E. A. Entemann, *J. Am. Chem. Soc.* **1961**, *83*, 3047–3050.
[41] N. C. Craig, L. G. Piper, V. L. Wheeler, *J. Phys. Chem.* **1971**, *75*, 1453–1460.
[42] T. Yamamoto, S. Tomoda, *Chem. Lett.* **1997**, 1069–1070.
[43] I. Novak, *J. Org. Chem.* **2000**, *65*, 5057–5058.
[44] Professor Ruben Contreras, University of Buenos Aires, private communication.
[45] M. J. Frisch, G. W. Trucks, H. B. Schlegel, G. E. Scuseria, M. A. Robb, J. R. Cheeseman, J. A. Montgomery Jr, T. Vreven, K. N. Kudin, J. C. Burant, J. M. Millam, S. S. Iyengar, J. Tomasi, V. Barone, B. Mennucci, M. Cossi, G. Scalmani, N. Rega, G. A. Petersson, H. Nakatsuji, M. Hada, M. Ehara, K. Toyota, R. Fukuda, J. Hasegawa, M. Ishida, T. Nakajima, Y. Honda,

O. Kitao, H. Nakai, M. Klene, X. Li, J. E. Knox, H. P. Hratchian, J. B. Cross, C. Adamo, J. Jaramillo, R. Gomperts, R. E. Stratmann, O. Yazyev, A. J. Austin, R. Cammi, C. Pomelli, J. W. Ochterski, P. Y. Ayala, K. Morokuma, G. A. Voth, P. Salvador, J. J. Dannenberg, V. G. Zakrzewski, S. Dapprich, A. D. Daniels, M. C. Strain, O. Farkas, D. K. Malick, A. D. Rabuck, K. Raghavachari, J. B. Foresman, J. V. Ortiz, Q. Cui, A. G. Baboul, S. Clifford, J. Cioslowski, B. B. Stefanov, G. Liu, A. Liashenko, P. Piskorz, I. Komaromi, R. L. Martin, D. J. Fox, T. Keith, M. A. Al-Laham, C. Y. Peng, A. Nanayakkara, M. Challacombe, P. M. W. Gill, B. Johnson, W. Chen, M. W. Wong, C. Gonzalez, J. A. Pople, *Gaussian03*, revision C.02, Gaussian, Inc., Wallingford, CT, **2004**.
[46] A. D. Becke, *J. Chem. Phys.* **1993**, *98*, 5648–5652.
[47] C. Lee, W. Yang, R. G. Parr, *Phys. Rev. B* **1988**, *37*, 785–789.
[48] A. E. Reed, F. Weinhold, *J. Chem. Phys.* **1983**, *78*, 4066–4073.
Received: May 28, 2006
Published Online: September 8, 2006

